

# Kinetics and Locus of Failure of Receptor-Ligand-Mediated Adhesion Between Latex Spheres. I. Protein-Carbohydrate Bond

David F. J. Tees and Harry L. Goldsmith

McGill University Medical Clinic, Montréal General Hospital Research Institute, Montréal, Québec H3G 1A4 Canada

**ABSTRACT** We previously described the use of a counter-rotating cone and plate rheoscope to measure the time and force dependence of break-up of doublets of spheroid, swollen, and fixed red cells (SSRC) cross-linked by monoclonal IgM antibody. It has been shown that doublet break-up can occur by extraction of receptors from the membrane, rather than by antibody-antigen bond break-up, and is a stochastic process. We therefore prepared 4.62- $\mu\text{m}$  carboxyl modified latex spheres with a covalently coupled synthetic blood group B antigen trisaccharide. Using a two-step carbodiimide process, ethylene diamine was covalently linked to the carboxyl modified latex spheres, and the trisaccharide, having an eight carbon spacer modified to bear a terminal carboxyl group, was linked to the ethylene diamine. Using these antigen spheres we carried out studies in Couette flow, in a transparent cone and plate rheoscope, of the shear-induced break-up of doublets cross-linked by monoclonal IgM anti-B antibody in 19% and 15% Dextran 40. As previously found with SSRC, over a range of normal force from 55 to 175 pN, there was a distribution in times to break-up. However, the fraction of antigen sphere doublets broken up, which increased from 0.08 to 0.43 at 75 pM IgM, and from 0.06 to 0.20 at 150 pM IgM, was significantly lower than that for the SSRC, where the fraction broken up at 150 pM IgM increased from 0.10 to 0.47. Thus, significantly higher forces were required to achieve the same degree of break-up for doublets of antigen-linked spheres than for SSRC. Computer simulation using a stochastic model of break-up showed that the differences between antigen sphere and SSRC doublet break-up were due to a change in bond character (the range and depth of the bond energy minimum) rather than to an increase in the number of bonds linking antigen-sphere doublets. This supports the notion that antibody-antigen bonds are ruptured in the case of antigen spheres, whereas antigen is able to be extracted from the membrane of SSRC, although changes of receptor substrate from cell to latex and the possibility of latex strand extraction from the microspheres are potential complicating factors.

## INTRODUCTION

Characterization of the physical strength of the bonds linking biological cells to each other and to surfaces is an important prerequisite for an understanding of adhesion processes such as cancer metastasis, platelet thrombosis, and leukocyte margination and extravasation. In recent years, the importance of the stochastic nature of break-up (Evans et al., 1991) has become apparent. For receptor-ligand bonds, the concept of a "force required to break a bond" loses much of its meaning. Interest has focused instead on the force dependence of the lifetime of a bond. If a bond is stressed, its lifetime (i.e., the average time needed for it to break stochastically) may either decrease, not change, or (paradoxically) increase (Dembo et al., 1988). Recent work on the phenomenon of neutrophil rolling has demonstrated that the kinetics of bond formation and dissociation are more important than the bond affinity (Lawrence and Springer, 1991). Adhesion of blood leukocytes to endothelial cells, the initial step in inflammation, is a multistep process. First, cells are seen to tether to and roll along endothelium in postcapillary venules. The rolling velocity

decreases until firm adhesion is achieved at the site of inflammation, allowing the cells to migrate through gaps between the endothelial cells and leave the circulation. The initial step in this process, rolling, has become the subject of a large literature since the discovery (Lawrence and Springer, 1991) that adhesion molecules which had appeared to be unimportant based on static assays of binding, the selectins, turned out to be essential for attachment in flow at physiological wall shear rates. Adhesion mediated by selectins is thought to be distinguished by very fast forward and reverse reaction rates compared to the more tenacious integrin mediated bonds, which are now thought to be responsible for the eventual arrest of cells once rolling has been initiated.

This new emphasis on rates has highlighted the lack of knowledge of the force dependence of bond kinetics. Bell (1978) developed an exponential model based on the kinetic theory of the strength of materials to describe the force dependence of the kinetics of bond formation and breakage. A bond is modeled as a free energy minimum of depth  $E_0$ . As the bond is stressed, the depth of the energy minimum is decreased by an amount  $r_0 \cdot f$ , where  $r_0$  is the range of the bond, representing the steepness of the energy minimum, and  $f$  is the applied force per bond. The minimum disappears completely when a "critical" value  $f_c = E_0/r_0$  is reached. A force of this magnitude will result in almost instantaneous bond failure. Bond break-up is still possible at forces less than  $f_c$ , however.

Received for publication 7 December 1995 and in final form 28 April 1996.

Address reprint requests to Dr. Harry L. Goldsmith, University Medical Clinic, Montréal General Hospital, 1650 Cedar Ave., Montréal, Québec H3G 1A4 Canada. Tel.: 514-937-6011, X2920; Fax: 514-937-6961; E-mail: mdhg@musica.mcgill.ca.

© 1996 by the Biophysical Society

0006-3495/96/08/1102/13 \$2.00

The equation relating the lifetime,  $t_b$ , to the force per bond is predicted to have the form (Bell, 1978)

$$t_b = \tau_o \exp(E_o - r_o \cdot f) / kT_K, \quad (1)$$

where  $\tau_o$  is the reciprocal of the natural frequency of oscillation of atoms in solids ( $\sim 10^{-13}$  s),  $T_K$  is the absolute temperature, and  $k$  is the Boltzmann constant. When  $f \ll E_o/r_o$ ,  $t_b \approx \tau_o \exp(E_o/kT_K)$ ; however, as the applied force increases to the "critical" value,  $f_c$ , the average time required to break up the bond decreases nonlinearly to a value on the order of  $\tau_o$ .

An alternative form for  $t_b$  has been proposed by Evans for forces sustained at a level near that required to rapidly rupture a bond, because at this force level, the decrease in  $E_o$  imparted by the force is likely to be strongly anharmonic:

$$t_b = \tau_o \left( \frac{f_o}{f} \right)^a. \quad (2)$$

In this empirical formula,  $\tau_o$  is again the time for rapid bond rupture,  $f_o$  is the force required to rapidly rupture a bond, and  $a$  characterizes the sensitivity of the bond to force:  $a \gg 1$  represents brittle bonds where rupture ensues swiftly as force is increased, whereas  $a \sim 1$  represents ductile bonds for which break-up increases very little as the force is increased (Evans, 1993).

Attempts have been made to determine experimentally the parameters in Bell's model. Kaplanski et al. (1993) used the arrest duration distribution of granulocytes rolling on interleukin 1-stimulated endothelial cells at extremely low flow rates [with hydrodynamic forces of 1–3 piconewtons (pN)] to measure the zero force bond lifetime,  $t_o$  [taken to be  $\tau_o \exp(E_o/kT_K)$ ]. The lifetime was found to be more than 200 times shorter than expected from measured reaction rates (between cell-bound receptors and soluble ligand), indicating a greater degree of reduction in bond lifetime with force than would be predicted by Bell's model. Investigators from the same laboratory recently determined the lifetime and two-state model kinetic constants of the bond between rabbit IgG2a coated on a latex sphere and glass surfaces derivatized with rabbit antindinitrophenol over a range of wall shear rates corresponding to forces between 5.6 and 37 pN acting on single bonds (Pierres et al., 1995). Alon et al. (1995), using neutrophils rolling along lipid bilayers containing P-selectin, were the first to measure the force dependence of the reverse rate constant for the P-selectin-carbohydrate ligand bond, using a method very similar to that of Kaplanski et al. (1993). They found  $r_o$  to be extremely small (only 0.05 nm), in keeping with other results (Dembo et al., 1988; Hammer and Apte, 1992) which suggest that the selectin protein-carbohydrate linkage is close to being an "ideal" bond, the lifetime of which varies very little with applied force (Dembo et al., 1988). By contrast, the value of  $r_o$  for a protein-protein bond is found to be larger (on the order of 0.3 nm), and the lifetime of the bond varies significantly with applied force (Erickson, 1994).

The models of Bell and Evans have also inspired work in our laboratory. Using a counter-rotating cone and plate rheoscope, which is able to generate virtually instantaneous uniform shear flow, Tees et al. (1993) studied the break-up of spheroid, swollen, and fixed red blood cells (SSRCs) agglutinated by monoclonal antibody. The elapsed time from the start of shear to break-up was measured over a range of applied hydrodynamic force from 30 to 200 pN. Forces were computed using previously derived equations for the normal force ( $F_n$ ) acting along and shear force ( $F_s$ ) acting normal to the doublet major axis in a linear shear field (Tha and Goldsmith, 1986), as given by

$$F_n = \alpha_3(h) \eta G b^2 \sin^2 \theta_1 \sin 2\phi_1, \quad (3)$$

$$F_s = \alpha_{12}(h) \eta G b^2 \sin \theta_1 \quad (4)$$

$$\times \left\{ \frac{(2 \sin^2 \theta_1 \cos^2 \phi_1 - 1)^2 \sin^2 \phi_1 + \cos^2 \theta_1 \cos^2 \phi_1}{1 - \sin^2 \theta_1 \cos^2 \phi_1} \right\}^{1/2}.$$

Here,  $\eta$  is the suspending medium viscosity,  $G$  the shear rate,  $b$  is the SSRC radius, and  $\theta_1$  and  $\phi_1$  are angles describing the orientation of the doublet major axis (Fig. 1);  $\alpha_{12}$  and  $\alpha_3$  are force coefficients that are weakly dependent on the minimum distance of approach,  $h$ , between sphere surfaces (for the SSRC,  $h = 20$  nm;  $\alpha_{12} = 19.33$  and  $\alpha_3 = 7.02$ ).

As expected, the bond lifetime decreased with applied force. To relate the force dependence of lifetimes of doublets to the force dependence of the reverse reaction rate ( $1/t_o$ ) of the bond, we used Bell's theory in a simulation of doublet break-up. The observed distribution of break-up

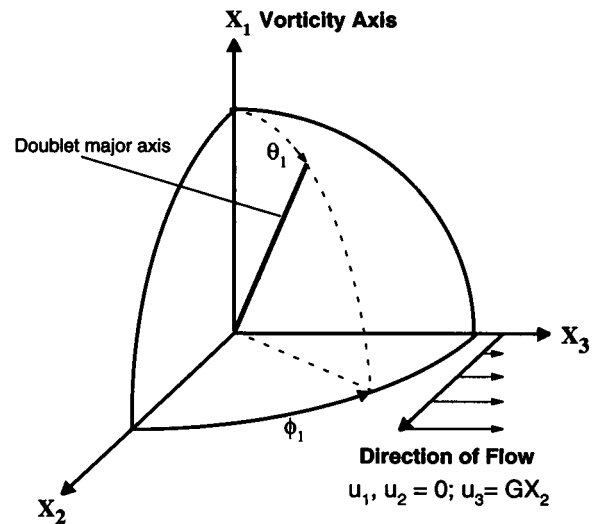


FIGURE 1 Cartesian,  $X_i$ , and spherical-polar ( $\theta_1$ ,  $\phi_1$ ) coordinates used to describe forces acting on doublets in a simple shear field. The  $X_3$  axis is the direction of flow, and  $X_1$  is the vorticity axis. The fluid velocity,  $u_i$ , has components in the  $X_3$  direction only, with  $u_3 = GX_2$ , where  $G$  is the shear rate. The heavy line represents the doublet major axis, which makes an angle  $\theta_1$  with respect to the vorticity,  $X_1$  axis, and the projection of which in the  $X_2X_3$  plane is at an angle  $\phi_1$  with respect to the  $X_2$  axis.

times could be well reproduced with an average of four bonds cross-linking the doublets.

There remained the question of the locus of bond rupture in the SSRC experiments. Evans et al. (1991) described a micropipette aspiration technique to join and then separate doublets of red blood cells, with one pressurized into a sphere, and the other glutaraldehyde-fixed. From studies of the transfer of fluorescent marker molecules during doublet separation, they demonstrated that it was possible to extract antigen from the membrane of the unfixed red blood cell. Subsequently, experiments in shear flow showed that blood group antigen extraction can occur, even with fixed red cells (Xia et al., 1994), which casts doubt on the assumption that break-up of the SSRC cross-bridge is due to failure of antigen-antibody bonds. We therefore embarked on experiments in which a synthetic blood group B antigen was covalently linked to latex microspheres. The spheres were cross-linked by the same monoclonal IgM antibody that was used in the SSRC study. Here, break-up of doublets of microspheres should occur through the rupture of antigen-antibody bonds and would be expected to result in a significantly different force dependence of doublet lifetime.

In this way, we hoped that the actual parameters for a protein-carbohydrate bond (blood group B antigen-antibody bond) could be determined. In the companion paper (Kwong et al., 1996), we describe a similar technique for studying the break-up of a protein-protein bond (protein G-IgG Fc domain bond).

## MATERIALS AND METHODS

### Synthetic blood-group B trisaccharide

A sample of the synthetic trisaccharide 2-*O*-( $\alpha$ -L-fucopyranosyl)-3-*O*-( $\alpha$ -D-galacto-pyranosyl)-(8-methoxycarbonyloctyl)- $\beta$ -D-galactopyranoside, the antigenic determinant of the blood-group B antigen (Lemieux and Driguez, 1975), was the gracious gift of Dr. David Rafter (Alberta Research Council, Edmonton, AB, Canada). The trisaccharide has an eight-carbon spacer, the 8-methoxycarbonyloctyl group, which facilitates binding to substrates. Samples of lyophilized antigen were dissolved in water to a concentration of 22 mM, and aliquots were stored at  $-20^{\circ}\text{C}$  until required for binding to latex microspheres. The methoxycarbonyl end group was converted to a carboxylic acid group (Lemieux et al., 1975) by incubating an aliquot in 0.1 N NaOH on a rotary mixer for 3 h at room temperature. The carboxylic acid end group could then be reacted with an amino group via the carbodiimide method described below.

### Antibodies

Monoclonal anti-blood group B and anti-blood group A affinity-purified mouse IgM antibody (DAKO Corporation, Dimension Labs, Mississauga, ON, Canada) were used for break-up experiments. For the (enzyme-linked immunosorbent assay) ELISA tests, alkaline-phosphatase conjugated polyclonal goat anti-mouse IgG + IgM(H + L) antibody (Jackson ImmunoResearch Labs, Bio/Can Scientific, Mississauga, ON, Canada) or polyclonal goat anti-mouse IgM ( $\mu$  chain) antibody (Sigma, St. Louis, MO) was used.

### Latex microspheres

Carboxyl modified latex (CML) surfactant-free polystyrene spheres of 4.97  $\mu\text{m}$  average diameter with high sphericity were used (Interfacial Dynamics

Corporation, Portland, OR). The particles are well characterized and have  $\sim 10^{10}$  carboxyl groups/sphere (measured by titration). There is also a much smaller number of residual sulfate groups ( $\sim 10^7$ /sphere). CML microspheres are produced from sulfate-stabilized spheres by a process of "grafting" or "entangling" polymers carrying large numbers of carboxyl groups onto the latex spheres. It is important to note that these groups reside in a three-dimensional surface coat, the thickness of which is dependent on the ionic strength of the suspending buffer. The very high density of carboxyl groups per unit area ( $\sim 10^3$   $\text{\AA}^2$ /charge group) therefore represents a radial rather than a two-dimensional distribution of charge groups within the surface coat. We estimate that at the ionic strength of 0.20 M phosphate-buffered saline (PBS), the spheres can approach to within  $h \approx 10$  nm, resulting in  $\alpha_{12}$  and  $\alpha_3 = 7.02$  and 19.24, respectively (showing that the coefficients are relatively insensitive to changes in  $h$ ).

The size distribution of a population of suspended particles measured under the microscope and with an aperture-impedance counter (Coulter Electronics, Hialeah, FL) was shown to be bimodal: 75% of spheres were  $4.63 \pm 0.10$   $\mu\text{m}$ , and 25% were  $5.57 \pm 0.12$   $\mu\text{m}$  in diameter. A small fraction (0.8%) of all particles were present as doublets or triplets when received. These aggregates were resistant to break-up under conditions of elevated pH (9–10), sonication, and hydrodynamic forces of at least 400 pN applied for 5 min.

### Coupling antigen to CML

Synthetic trisaccharide antigen was coupled to a CML particle by means of a two-step process. In the first step, a fraction of the carboxyl groups on the surface of the CML sphere were bound to ethylene diamine by using the water-soluble 1-ethyl-3-(3-dimethylaminopropyl) carbodiimide to activate the carboxyl groups on the sphere. Briefly,  $1.5 \times 10^9$  spheres were washed six times with ion-free water and reacted with 0.32 mM ethylene diamine and 0.32 mM carbodiimide in a 5-ml volume at the optimum pH of 6.5. After the suspension was mixed for 20 h at room temperature, the spheres were washed six times with deionized water and stored in 0.1%  $\text{NaN}_3$  to inhibit bacterial growth during storage. In the second step, the ethylene diamine linked spheres were coupled to antigen. Here,  $1.9 \times 10^8$  spheres were washed six times and reacted with 0.2 mM trisaccharide and 0.2 mM carbodiimide in a 1-ml volume at pH 6.5. After the suspension was mixed for 24 h at room temperature, spheres were finally washed six times with deionized water and stored in 0.1%  $\text{NaN}_3$  for at most 1 month before use.

### Characterization of antigen attachment to CML

The resulting spheres showed extensive agglutination (up to 31% of spheres in aggregates) when sheared at  $G = 8$   $\text{s}^{-1}$ , in a suspension containing 5000 spheres/ $\mu\text{l}$  with 75 pM anti-B antibody. By contrast, only background levels of aggregation (0.8%) were observed when the spheres were sheared with the same concentration of anti-A antibody.

Measurements of the electrophoretic mobility using a vertically mounted flat microelectrophoresis cell (Shaw, 1969) showed that the zeta potential of bare CML =  $-78$  mV decreasing to  $-68$  mV for the ethylene diamine linked spheres and to  $-58$  mV for the antigen spheres. This would indicate that only  $\sim 10\%$  of the carboxyl groups are coupled to ethylene diamine, corresponding to  $<10^9$  antigen groups per sphere.

The presence of bound antigen was verified by ELISA. Antigen spheres at a concentration of  $2 \times 10^5$  spheres/ $\text{ml}^{-1}$  were washed four times with 1% albumin/PBS (pH 7.4) and then incubated for 30 min at  $4^{\circ}\text{C}$  with 8.5  $\mu\text{g}/\text{ml}^{-1}$  of either anti-B or anti-A IgM (positive control) or with no first antibody (negative control). The spheres were washed five times and then resuspended in 300  $\mu\text{g}/\text{ml}^{-1}$  alkaline phosphatase-conjugated anti-mouse antibody for 30 min at  $4^{\circ}\text{C}$ . The spheres were washed five times more and then resuspended in 1  $\text{mg}/\text{ml}^{-1}$  of Sigma 104 (*p*-nitrophenyl phosphate, disodium, hexahydrate; a generous gift of Dr. Gerald Price, McGill Cancer Centre), the substrate for alkaline phosphatase, in 1 M diethanolamine buffer (pH 9.8) and left to incubate at  $4^{\circ}\text{C}$  for 35 min. The reaction was quenched with 5 N NaOH, and the optical density at 405 nm ( $\text{OD}_{405}$ ) of the sphere supernatants was measured in a spectrophotometer. With the anti-A

antibody, the OD<sub>405</sub> was indistinguishable from samples of spheres with no first antibody added. With the anti-B antibody, however, a signal of up to 10× background was found. In the absence of carbodiimide during the linking of antigen to the ethylene diamine-linked spheres, both agglutination and ELISA tests showed only background levels of aggregation, as did tests of carbodiimide linking of antigen to bare CML spheres. The binding of the antigen to the spheres would thus seem to be due to a covalent bond and not to nonspecific adsorption.

### Maximum number of bonds

Using another ELISA, the amount of antibody bound to the spheres was measured. Samples of antigen-linked spheres were incubated at  $5 \times 10^3$  spheres·μl<sup>-1</sup> with 75 or 150 pM IgM anti-B antibody, and then the spheres were washed and concentrated. A series of sphere concentrations were incubated with alkaline phosphatase-conjugated anti-IgM second antibody at 37°C for 2 h and then developed with Sigma 104 for 15 min. The OD<sub>405</sub> was measured and compared with a standard curve made by incubating various concentrations of anti-B antibody, bound to unlabeled goat anti-mouse IgM-coated microtiter plate wells. The wells were incubated at 37°C for 2 h with alkaline phosphatase-conjugated second antibody as above and then developed with Sigma 104 for 15 min. Once developed, the OD<sub>405</sub> was used as a standard curve to determine the amount of anti-B antibody bound to the spheres. The spheres incubated in 75 and 150 pM anti-B IgM were found to have 1600 and 2300 IgM molecules/sphere, respectively.

An estimate of the upper limit on the number of cross-bridges between antigen-linked sphere doublets can be made from the concentration of bound antibody. As determined above, in a suspension containing 150 pM IgM, an average of 2300 antibody molecules are available for binding to each sphere. The mean surface area of the antigen-linked sphere is 68 μm<sup>2</sup>. Assuming that the bonding surfaces are separated by a minimum of 10 nm and a maximum of 45 nm (determined by the size of an IgM molecule; Tha and Goldsmith, 1986), the maximum area for sphere cross-linking by IgM (given by the surface area of the spherical cap,  $2\pi r_j h$ , of thickness  $j = [45 \text{ nm} - 10 \text{ nm}]/2 = 17.5 \text{ nm}$ ) is 0.25 μm<sup>2</sup>. Even at 150 pM IgM (the highest concentration used in the experiments described below), the average number of antibodies in the region of cross-linking would be ~8 on each of the cells of a doublet, making a maximum of 16 possible bonding molecules. Because the spheres bear at most 10<sup>9</sup> blood group B antigen sites on their surface as determined by electrophoresis, there will be ~10<sup>5</sup> sites in the 0.25 μm<sup>2</sup> contact area on each cell. Clearly, therefore, the number of cross-bridges is greatly limited by the amount of antibody available for bonding. Sixteen bonds is probably an overestimate of cross-linking, partly because not all the antibody will participate in cross-linking the spheres, and partly because many of the antibody molecules in the region of binding will be multiply linked to antigens on their own sphere. Consequently, the number of cross-bridges linking the latex spheres is likely to be small, and as low as one or two in some cases, a hypothesis supported by the low frequency of doublet formation in collisions between latex particles, as also found in the case of the SSRC (Tees et al., 1993), even though the number of antigen sites for the latex spheres is estimated to be much higher than for the SSRC (~10<sup>6</sup> per cell, and  $2 \times 10^3$  in the contact area). In both systems, the antigen site density is very large compared to the number of antibody molecules available for binding.

### Rheoscope

As previously described (Tees et al., 1993), force application experiments were carried out using a transparent, counter-rotating cone and plate rheoscope system (model MR-1; Myrenne Instruments, Fremont, CA) mounted on a Leitz Diavert inverted microscope (Ernst Leitz Ltd., Midland, ON, Canada). Because the cone and plate counter-rotate at the same angular velocity,  $\Omega$ , there is a layer of zero translational velocity located in the midplane of the gap, in which doublets can be viewed for extended periods of time. Particle motions were observed and recorded at radial distances of 0.7 to 1.0 mm from the center of rotation, using a CCD video

camera (model AVC-D7; Sony Canada, Ltd., Montréal, QC, Canada). A digital time display was added to the resulting video images, and the output was recorded on videotape for analysis off-line.

For the cone and plate geometry, the shear rate is independent of distance from the cone center, and is given by  $G = 2\Omega/\tan \psi$ , where  $\psi$  is the cone angle (nominally 2°, and measured using a digital gauge as  $2.1 \pm 0.1^\circ$ ). The rheoscope cone and plate angular velocity, and hence  $G$ , is adjusted by using a 10-turn variable resistor. After several months of use, remeasurement of the cone and plate gap at various radial distances from the cone center revealed some flattening of the center of the acrylic cone. To account for this, a modified equation for the shear rate was used:

$$G = \frac{2\Omega}{\tan \Psi} \left( 1 + \frac{d}{R} \right), \quad (5)$$

where  $d$  is the radius of the flattened portion of the cone center (0.18 mm), and  $R$  is the distance from the cone center. Far from the cone center, this equation reduces to the equation for an ideal cone.

Doublets of spheres formed in the rheoscope rotate with a period of rotation  $T$  (Goldsmith and Mason, 1967):

$$T = \frac{2\pi}{G} \left( r_c + \frac{1}{r_c} \right), \quad (6)$$

where  $r_c$ , the axis ratio of the ellipsoid having the same  $T$  as a doublet of touching rigid spheres, equals 1.98 (Wakiya, 1971). The predicted dimensionless period of rotation for the doublet,  $TG$ , is therefore 15.61. As a check on the applicability of Eq. 5, the periods of rotation of 36 doublets were measured at the lowest shear rate possible ( $8 \text{ s}^{-1}$ ), and  $TG$  was computed using values of  $G$  from Eq. 5 with  $\psi = 2^\circ$ . A mean value for  $TG$  of  $15.6 \pm 1.1$  (SD) was found, in good agreement with that predicted by theory, 15.61. The sizable error in  $TG$  is due principally to measured variations of  $\pm 10\%$  in  $\Omega$ . Because of the fact that there was significant flattening of the cone and changes in cone angle over extended periods, the local shear rate for each doublet was determined from the period of rotation.

### Data acquisition

As in previous work (Tha et al., 1986; Tees et al., 1993), the results are given in terms of the maximum normal force acting on a doublet in the final half-orbit before break-up (Eq. 3), computed using the following equation relating  $\theta_1$  to  $\phi_1$  (Goldsmith and Mason, 1967):

$$\tan \theta_1 = \frac{Cr_c}{(r_c^2 \cos^2 \phi_1 + \sin^2 \phi_1)^{1/2}}, \quad (7)$$

the equation of a spherical ellipse, the eccentricity of which is defined by the orbit constant  $C$ , with the experimentally determined values of  $\eta$ ,  $G$ ,  $b$ , and  $\theta_1$ .

As mentioned above, the latex microspheres are bidisperse. Because the theory described in Eq. 3 above applies only to doublets of equal-size spheres, only doublets of small or large spheres were chosen for break-up experiments.

### Suspensions for break-up experiments

In the previous work with SSRC in the rheoscope (Tees et al., 1993), the suspending medium was 52% sucrose ( $\eta_{23^\circ\text{C}} = 18.6 \text{ mPa}\cdot\text{s}$ ). Despite an appreciable particle-suspending phase density difference,  $\Delta\rho = -0.140 \text{ g}\cdot\text{cm}^{-3}$ , no significant sedimentation was observed over the course of several hours. This was likely due to diffusion of suspending phase into the SSRC. In the case of the polystyrene spheres,  $\Delta\rho = -0.195 \text{ g}\cdot\text{cm}^{-3}$ , the rate of sedimentation in sucrose,  $\sim -0.14 \mu\text{m}\cdot\text{s}^{-1}$ , was too rapid to allow studies of doublet break-up to be carried out. To reduce sedimentation to an acceptable level, we chose Dextran 40 as the viscous cosolvent. Antigen-linked spheres

were suspended at a concentration of  $5 \times 10^3$  particles  $\mu\text{L}^{-1}$  in 19% Dextran 40 in PBS with 0.5% bovine serum albumin to inhibit nonspecific adhesion (pH 7.1);  $\Delta\rho = -0.026 \text{ g cm}^{-3}$ ,  $\eta_{23^\circ\text{C}} = 18.3 \text{ mPa}\cdot\text{s}$ , the latter closely matching the viscosity of 52% sucrose. Anti-B IgM was added at final concentrations of 75 or 150 pM, and the suspension was placed on a rotary mixer for 1 h before the start of break-up experiments. All experiments were performed at room temperature (22–24°C).

For studies at lower viscosity, 15% Dextran 40 ( $\eta_{23^\circ\text{C}} = 9.7 \text{ mPa}\cdot\text{s}$ ;  $\Delta\rho = -0.014 \text{ g cm}^{-3}$ ) was used as the viscous cosolvent. For studies on the effect of pH, the suspending medium pH was adjusted to 5.8 or 7.8.

## Rheoscope protocol

Fifty microliters of fresh antigen-sphere/antibody suspension was pipetted into the rheoscope. Doublets were allowed to form as a result of two-body collisions at the lowest  $G = 8 \text{ s}^{-1}$  (corresponding to  $F_{n, \text{max}} \approx 17 \text{ pN}$ , for  $C = \infty [\sin^2\theta_1 \sin 2\phi_1 = 1.0]$  and  $\eta = 18 \text{ mPa}\cdot\text{s}$ ), and after the rotational orbit of a doublet found close to the midplane was analyzed, the rheoscope variable resistor speed setting required to produce the desired force was determined, as previously described (Tees et al., 1993). The doublet was then observed and videotaped at the preset shear rate until break-up or until it disappeared from view. If break-up was recorded in the video camera field of view, the time to break-up from the start of flow,  $t_b$ , could be measured to within 1–2 video frames,  $\pm 0.06 \text{ s}$ . For the 20% of doublets for which break-up was observed through the microscope, but outside the video camera field of view, the time of break-up was signaled by stopping the rheoscope motion, resulting in a value of  $t_b$ , from which the observer reaction time (measured to be 0.8 s) was subtracted.

The small remaining buoyancy of the antigen spheres resulted in particles taking  $\sim 30 \text{ min}$  to rise from near the bottom plate to above the layer of no translation in the midplane. Consequently, the rheoscope was refilled every half-hour, and only one doublet was recorded per filling. This protocol ensured that no doublet was measured twice, and none were exposed to high shear rates until the moment of application of shear. Furthermore, the frequent refilling allowed recently formed doublets to be identified: any preexisting doublet traveling close to the plate would appear within  $\sim 1$  rotation of the instrument after initiation of slow flow; accordingly, doublets were only sought after observation of one instrument rotation had confirmed that no preexisting doublets were present, ensuring that doublets subsequently observed near the plate had recently formed in the rheoscope. Doublets so identified were allowed to rise under no-flow conditions until they reached the median plane, at which point they were sheared. This procedure should have reduced the number of nonspecific doublets inadvertently analyzed. Counts of the number of doublets in a population of spheres with anti-B and anti-A antibody in the rheoscope showed that  $\sim 2\%$  of doublets (but  $<1\%$  of all spheres) in a filling were nonspecifically bound. Other than the protocol for finding recently formed doublets, no other precautions were taken, but because it was shown that preexisting, nonspecifically bound doublets could not be broken, even by extremely large forces, their inclusion would only slightly decrease the fraction of doublets broken up.

Approximately 7% of the break-ups observed had to be discarded, because of interactions with spheres close to the doublet that might have been the cause of break-up.

## Computer simulation

A Monte Carlo simulation of doublet break-up was used to relate the results of doublet break-up experiments to the force dependence of the reverse reaction rate constant,  $k_{\text{off}}$ . The method was that described by Tees et al. (1993), with minor modifications.

If, following Bell (1978), we make the identification  $k_{\text{off}} = 1/t_b$ , the probability of bond breakage,  $P_b$ , in a short time interval,  $\Delta t$ , has been shown to be (Hammer and Apte, 1992)

$$P_b = 1 - \exp(-k_{\text{off}}\Delta t) = 1 - \exp\left[-\frac{\exp(c \cdot f)}{t_o} \Delta t\right]. \quad (8)$$

where a simplified expression for Eq. 1,  $t_b = t_o \exp(-c \cdot f)$ , has been used.

In the simulation,  $t_o$  and  $c$  are parameters to be varied to fit the data. The number of bonds,  $N_b$ , holding the spheres together, chosen for each simulated doublet from a Poisson distribution (Capo et al., 1982), must also be provided, because it is necessary for the computation of  $f$ , the force per bond. The shear rate required to achieve a chosen maximum value of  $F_n$  was determined for a randomly chosen orbit constant. The period of rotation was found from the shear rate using Eq. 6. Each rotation was divided into  $N_s$  equal time steps of duration  $\Delta t = T/N_s$ ; here  $N_s$  was chosen to be 1000. The viscosities were taken to be 18 and 10 mPa·s, equal to those of 19% and 15% Dextran 40 at 23°C, respectively. For each time step,  $P_b$  was computed from Eq. 8 using the chosen values of  $c$  and  $t_o$ , and the force per bond calculated with Eq. 3 for the current instantaneous values of  $\phi_1$ ,  $\theta_1(\phi_1, C)$ ,  $G$ , and  $N_b$ . A random number between 0 and 1 was chosen from a uniform distribution for each bond remaining. If the number drawn for a bond was less than  $P_b$ , the number of bonds was reduced by one, and the force per bond acting on the remaining bonds was recalculated. Thus, sequential bond failure is an inherent feature of the model. Bond formation (independent of force) was included in the simulation by the incorporation of a bond formation time  $t_f$ . At each time step a test for bond formation was made. The cycle of probability calculation, formation, and break-up testing was repeated, until the number of bonds was reduced to zero, or 10 rotations had elapsed, because only the first 10 rotations are considered in the experiments described below.

The bond parameters supplied to the simulation are  $t_o$ ,  $t_f$ ,  $c$ , and the average value of the Poisson distribution of the bonds linking the cells,  $\langle N_b \rangle$ . The simulated experimental variables supplied were the maximum normal force,  $F_{n, \text{max}}$ , and the number of simulated doublets,  $n$ . The bond parameters were varied under simulated experimental conditions resembling those in the rheoscope in an attempt to achieve a match to the experimental data.

## Error analysis

### Viscosity

Temperature fluctuations of  $\pm 0.1^\circ\text{C}$  over the course of a doublet tracking account for an error of  $\pm 0.1 \text{ mPa}\cdot\text{s}$ ,  $<1\%$  of the viscosity of the suspending media used. Because an individual filling lasted for less than 30 min, any increase due to evaporation was negligible.

### Particle diameter

The standard deviation in  $2b$  was measured to be  $\pm 0.1 \mu\text{m}$  from an analysis of 50  $4.63\text{-}\mu\text{m}$  spheres. This amounts to a 2% error in diameter.

### Angle factors

Here, errors arise from uncertainty in the computation of the orbit constant,  $C$ , which in turn depends on errors in the measured projected doublet axis length. These errors decreased from 5% to 2.5% as  $C$  decreased from 10 to 1. For values of  $C > 5$ , when  $\theta_1$  is close to  $90^\circ$  throughout the orbit, the above errors lead to very small differences in the maximum value of the angle factor. Calculations show that the maximum error was  $\sim \pm 3\%$ .

### Shear rate

The error in  $G$  depends on the uncertainty in measuring the period of rotation  $T$  (Eq. 6), because most estimates of  $G$  were done using  $TG = 15.61$ . Because the doublets were observed over three to five orbits (a period of 0.25–3 s), and the number of orbits was determined to within one videotape frame (0.03 s), the error in  $T$ , and hence  $G$ , was at most 5%. In cases where the doublet broke up within one rotation, Eq. 5 was used to calculate  $G$ ; here, the principal error source was the systematic error due to variation in the cone and plate rotation speeds over the course of a cone and plate rotation. There were excursions of up to 10% in the shear rate over the course of a minute. Because very few doublets were in view for more

than a few seconds, this is only a serious source of error for the very long-lasting doublets, and not for those seen for less than 10 rotations, the population used in the Results section.

The above errors were propagated through the force calculations for individual break-ups. Calculations with standard formulae for independent errors (Bevington, 1969) show that the total error in the computed forces varied from  $\pm 10\%$  to  $\pm 20\%$ .

## RESULTS

The applied force acting on the doublets varies periodically (Eqs. 3 and 4); the particles were subjected to two periods of tensile and two periods of compressive stress in each orbit. The number of rotations executed by a doublet from the onset of shear in time  $t$  ( $= t/T$ ) gives the number of times it has been exposed to a given force. Accordingly, the results of the temporal distribution of break-up below have been standardized by plotting times as the dimensionless number of rotations.

The period of rotation of a doublet decreases with increasing shear rate (Eq. 6), but the time taken to traverse the field of view and be lost also decreases with shear rate. The combination of these two effects results in the number of rotations for which a doublet is visible being roughly constant ( $\sim 10$  rotations) at all forces. Because very few doublets broke up (or were visible) beyond 10 rotations, the break-up statistics were compiled from those doublets that broke up within 10 rotations of the onset of flow.

### Temporal distribution of break-up

The number of rotations to break-up or loss from the field of view in the rheoscope was determined for all doublets examined. Fig. 2, *a* and *b*, shows the fraction of doublets that broke up in a given rotation, i.e., the fraction of the total number of doublets observed in that rotation that broke up plotted against the elapsed number of rotations for 75 and 150 pM IgM, respectively. The data were binned into four force ranges:  $30 \leq F_n < 85$  pN,  $85 \leq F_n < 145$  pN,  $145 \leq F_n < 205$  pN, and  $205 \leq F_n < 265$  pN. In the two lowest force ranges at both [IgM], the fraction of break-ups is very low and there is very little variation with time after the onset of shear. With increasing force, however, there is an increase in the fraction of break-ups and, particularly at 75 pM IgM, there is a bias toward break-up occurring in the first three rotations. Thus, at 75 pM IgM, the fraction of doublets breaking up in the first rotation increased from 14% to 21% in going from the 145–205 pN to the 205–265 pN range, and in both ranges the fraction breaking up in the fourth rotation had fallen to 3%. In contrast, at 150 pM IgM, the fraction breaking up increased from 4.1% to 6.2% in the first rotation and remained effectively constant over the first four rotations.  $\chi^2$  tests of significance (Press et al., 1986) show that between the 75 pM and 150 pM data, the low force values are indistinguishable ( $p \sim 0.50$ ), but that the two higher force curves are significantly different ( $p < 0.05$ ).

In addition to the temporal distribution of break-ups, two aggregate statistics can be calculated. The average number

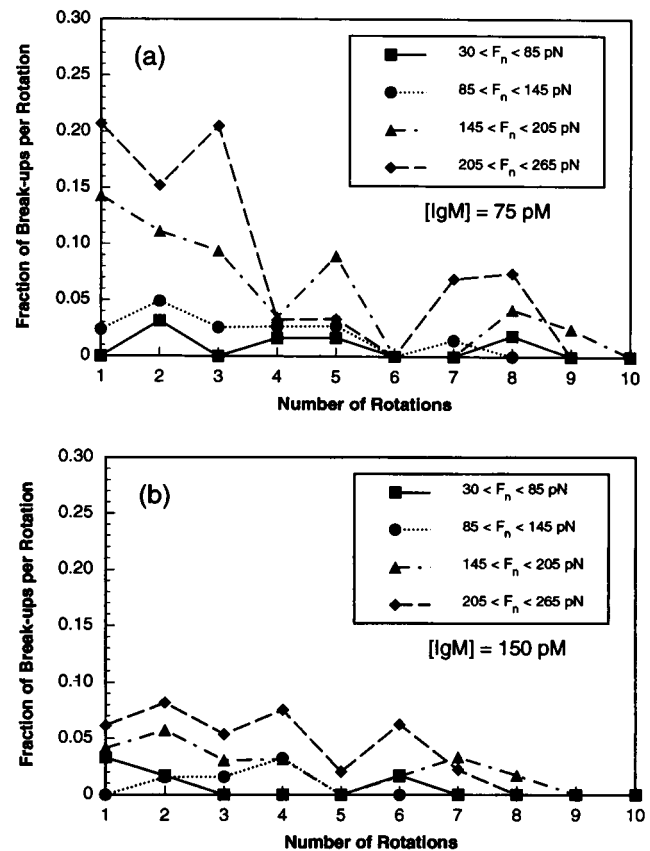


FIGURE 2 Graph of fraction of break-ups per rotation (the fraction of the total number of doublets observed in that rotation which broke up after the onset of shear) for latex spheres in 19% Dextran 40 over four force ranges. (a) 75 pM IgM; (b) 150 pM IgM.

of rotations before break-up,  $\langle N_r \rangle$ , for doublets broken within 10 rotations is shown in Table 1 for the 75 and 150 pM data in the four force ranges. Although there is a slight trend toward fewer rotations (and hence more rapid break-up) with increasing force for the 75 pM data, this change is not significant, and in fact none of the differences in  $\langle N_r \rangle$  are significant between different forces or between the two [IgM].

TABLE 1 Average number of rotations to break-up for doublets breaking within 10 rotations

Applied force (pN)	$\langle N_r \rangle \pm \text{SD}, s$	
	75 pM IgM	150 pM IgM
$30 \leq F_n < 85$	$3.6 \pm 2.2$ ( $n = 5$ )	$1.8 \pm 2.4$ ( $n = 4$ )
$85 \leq F_n < 145$	$2.6 \pm 1.7$ ( $n = 13$ )	$2.7 \pm 1.2$ ( $n = 4$ )
$145 \leq F_n < 205$	$2.4 \pm 2.2$ ( $n = 36$ )	$3.0 \pm 2.4$ ( $n = 15$ )
$205 \leq F_n < 265$	$2.2 \pm 2.0$ ( $n = 33$ )	$2.8 \pm 1.7$ ( $n = 21$ )

All comparisons are not significantly different.  
 $n$ , Number of break-ups.

Table 2 shows the fraction of all doublets observed in the force range that broke up within 10 rotations. As was apparent from the distribution data, for both [IgM], the fraction broken up increases with increasing applied force. In addition, the values at 150 pM are less than those at 75 pM in each force range, indicating that in the presence of more antibody, fewer doublets are broken up. A combination of the fourfold tables for comparison of the series of percentages that went into this table (Sachs, 1984), yields a standard normal estimate which reveals that the 75 pM and 150 pM break-up fractions are highly significantly different ( $p \ll 0.01$ ).

### Effect of viscosity

In the previous work with SSRC in a constantly accelerating Poiseuille flow (Tha et al., 1986; Tees et al., 1993), a small viscosity-dependent increase in the average force at the moment of break-up was observed. This was ascribed to an artifact of the doublet selection process (the higher force generated by the higher viscosity medium was posited to break up doublets bound by few bonds before they could be observed, thus biasing the forces toward doublets linked by larger numbers of bonds). There remained some suspicion as to whether there might be an effect of viscosity on the strength or number of bonds, especially in view of the work of Yedgar and others (Almagor et al., 1992) on the effect of viscosity on the kinetic coefficients of ligand-protein interactions and subsequent biochemical processes. However, in our system, the effect of medium viscosity is more likely to manifest itself through changes in the ligand and receptor diffusivity, and therefore the antibody-antigen bond formation rate, rather than through changes in the nature of the receptor-ligand detachment mechanism and the off rate constant. Thus, the number of cross-bridges and doublets formed during shear at low  $G$  is expected to decrease with increasing viscosity.

To examine the effect of viscosity, a series of experiments were performed using 15% Dextran 40 ( $\eta_{23^\circ\text{C}} = 9.7$  mPa·s) instead of 19% Dextran 40 ( $\eta_{23^\circ\text{C}} = 18.3$  mPa·s) at 75 pM IgM. Too few data were generated to analyze the temporal distribution of break-ups per rotation, but the

aggregate statistics were computed and compared with the 19% Dextran data.

Table 3 shows that the values of  $\langle N_r \rangle$  are slightly lower in 15% Dextran than in 19% at all force ranges, although this difference is only statistically significant for the lowest force range (probably because of the small number of break-ups in the 15% Dextran in this range). As with the 19% Dextran, the differences in  $\langle N_r \rangle$  between force ranges at a given [IgM] are not statistically significant.

By contrast, the fraction of doublets broken within 10 rotations, shown in Table 4, is markedly smaller than that in 19% Dextran in all three force ranges at 75 pM IgM, and as before, the fraction of doublets broken up within 10 rotations increases with increasing force. Using a comparison of fourfold tables as above, the difference between the two columns is highly significant ( $p < 0.001$ ). It is interesting to note, however, that a similar comparison with the 150 pM 19% Dextran data reveals no significant difference ( $p \sim 0.40$ ).

### Dependence of break-up on pH

Concern over the locus of failure of the attachment led us to seek confirmation of antigen-antibody bond breakage, even with antigen covalently coupled to microspheres. If an antigen-antibody bond is being broken, doublet break-up should become more frequent as suspending medium pH is lowered, because of weakening of electrostatic interactions (van Oss and Absolom, 1984; Cozens-Roberts et al., 1990). Accordingly, the pH dependence of the fraction of doublets broken up within 10 rotations in the usual force ranges was determined. The pH of the final Dextran suspensions used was 5.8, 7.1, and 7.8. As shown in Table 5, there was a significant ( $p < 0.01$ ) increase in the fraction of break-up with the reduction of pH from 7.8 to 7.1. Strangely, however, there was almost no break-up at pH 5.8 for these spheres (only two of 34 doublets in all force ranges).

## DISCUSSION

The objective of the work reported here was to establish whether the time and force dependence of break-up of

**TABLE 2** Fraction of doublets breaking up within 10 rotations

Applied force (pN)	Fraction of break-ups	
	75 pM IgM	150 pM IgM
$30 \leq F_n < 85$	0.08 ( $n = 64$ )	0.06 ( $n = 61$ )
$85 \leq F_n < 145$	0.16 ( $n = 84$ )	0.06 ( $n = 64$ )
$145 \leq F_n < 205$	0.43 ( $n = 84$ )	0.20 ( $n = 73$ )
$205 \leq F_n < 265$	0.57 ( $n = 58$ )	0.37 ( $n = 65$ )

$n$ , Number of doublets.

**TABLE 3** Effect of viscosity: comparison of the average number of rotations to break-up,  $\langle N_r \rangle$ , for doublets breaking up within 10 rotations in 15% and 19% Dextran for 75 pM IgM

Applied force (pN)	$\langle N_r \rangle \pm \text{SD}, s$	
	19% Dextran	15% Dextran
$85 \leq F_n < 145$	$2.6 \pm 1.7^*$ ( $n = 13$ )	$1.1 \pm 0.8^*$ ( $n = 3$ )
$145 \leq F_n < 205$	$2.4 \pm 2.2$ ( $n = 36$ )	$2.2 \pm 1.7$ ( $n = 11$ )
$205 \leq F_n < 265$	$2.2 \pm 2.0$ ( $n = 33$ )	$1.6 \pm 1.9$ ( $n = 4$ )

\* $p < 0.05$ ; all other comparisons are not significantly different.

$n$ , Number of break-ups.

**TABLE 4** Effect of viscosity: comparison of the fraction of doublets breaking up within 10 rotations in 15% and 19% Dextran for 75 pM IgM

Applied force (pN)	Fraction of break-ups	
	19% Dextran	15% Dextran
$85 \leq F_n < 145$	0.16 ( $n = 84$ )	0.12 ( $n = 39$ )
$145 \leq F_n < 205$	0.43 ( $n = 84$ )	0.17 ( $n = 66$ )
$205 \leq F_n < 265$	0.57 ( $n = 58$ )	0.36 ( $n = 11$ )

$n$ , Number of doublets.

doublets of latex spheres bearing covalently bound antigen is significantly different from that previously found for doublets of SSRC, in an attempt to resolve the question of whether break-up is due to an antigen-antibody bond being broken or to extraction of the antigen from the membrane of the red blood cell.

Data were previously obtained with SSRC in 52% sucrose, which has a viscosity at 23°C almost identical to that of 19% Dextran (Tees et al., 1993). Concern over the possible effect of a change of suspending medium from sucrose to Dextran led to a repeat of SSRC doublet break-up experiments in 19% Dextran 40. Fig. 3, *a* and *b*, shows the temporal distribution of break-up of the SSRC at 150 pM IgM for 52% sucrose (rebinned from Tees et al., 1993, to the same force ranges as in Fig. 2) and 19% Dextran 40, respectively. It is evident that the two sets of SSRC curves are very similar; both show a much larger fraction of break-up in the first rotation in the two highest force ranges than those for antigen sphere doublets. Table 6 compares the fraction of SSRC breaking up within 10 rotations at 75 and 150 pM IgM in sucrose, and at 150 pM IgM in Dextran, with the fraction of antigen sphere doublets broken up. The table reveals that the fraction of break-ups of SSRC doublets is significantly greater than that of antigen sphere doublets, even when the effect of changing suspending medium from sucrose to Dextran is considered, an observation borne out by comparison of combined fourfold tables ( $p < 0.01$ ) at both 75 and 150 pM IgM. With increasing force, not only do the SSRCs exhibit a greater increase in the fraction of break-ups in the first rotation than do the latex spheres, but the SSRCs also exhibit a much faster

**TABLE 5** Effect of suspending medium pH on the fraction of doublets breaking up within 10 rotations

Applied force (pN)	Fraction of break-ups		
	pH 5.8	pH 7.1	pH 7.8
$85 \leq F_n < 145$	0.00 ( $n = 10$ )	0.16 ( $n = 84$ )	0.06 ( $n = 17$ )
$145 \leq F_n < 205$	0.12 ( $n = 16$ )	0.43 ( $n = 84$ )	0.20 ( $n = 45$ )
$205 \leq F_n < 265$	0.00 ( $n = 8$ )	0.57 ( $n = 58$ )	0.52 ( $n = 21$ )

$n$ , Number of doublets.

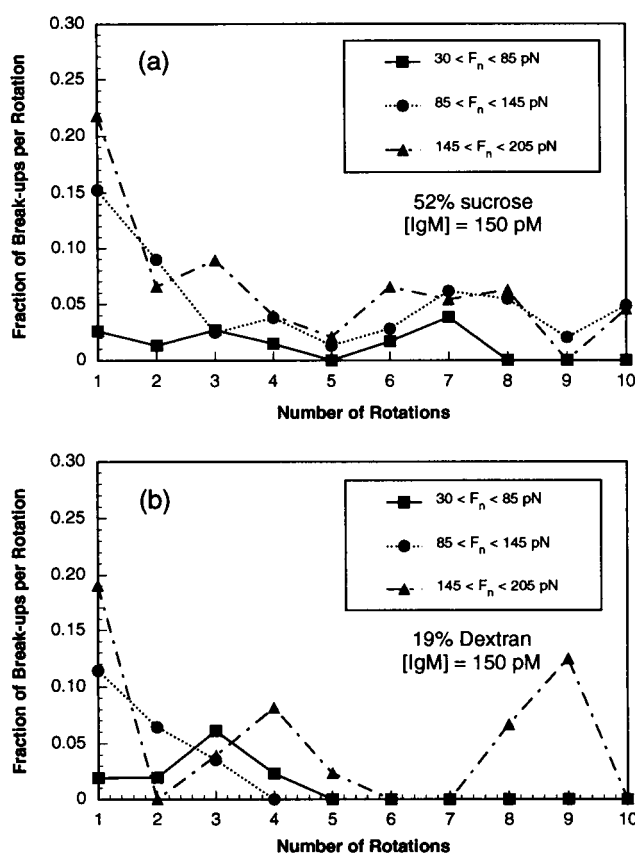


**FIGURE 3** Graph of fraction of break-ups per rotation for doublets of SSRC in (a) 52% sucrose with 150 pM IgM over three force ranges (rebinned from Fig. 6 in Tees et al., 1993) and (b) 19% Dextran 40 with 150 pM IgM over three force ranges.

decay in fraction of break-ups with time.  $\chi^2$  tests show the curves in Fig. 3 *a* to be significantly different from both the 150-pM IgM (Fig. 2 *b*;  $p < 0.01$ ) and the 75-pM latex sphere curves (Fig. 2 *a*;  $p < 0.05$ ).

These differences show that doublets of latex microspheres with covalently coupled antigen are significantly harder to break up than the doublets of SSRCs. One possible reason for this difference is that the number of bonds linking doublets of antigen spheres is greater than that linking doublets of SSRC. A second possibility is that the strength of the bond itself is greater.

### Monte Carlo simulation

To distinguish whether bond number or bond character is responsible for the different patterns of adhesion observed for antigen spheres and SSRC, a Monte Carlo simulation of doublet break-up in shear flow using the theory of Bell (1978) was performed as described in Materials and Methods. The simulation was similar to that in Tees et al. (1993), except that the possibility of bond formation was included. The model used four parameters: 1)  $c$ , a parameter related to the range of the bond ( $= r_0/kT_K$ ); 2)  $t_0$ , the average break-up time at zero force [ $= \tau_0 \exp(E_0/kT_K)$ ]; 3)  $t_f$ , the average time



**TABLE 6** Effect of viscous co-solvent: comparison of the fraction of doublets breaking up within 10 rotations for SSRC in 52% sucrose (rebinned from Tees et al., 1993), with that in 19% Dextran, both compared with the fraction of doublets of antigen-linked spheres breaking up at 75 and 150 pM IgM

Applied force (pN)	Fraction of break-ups				
	Latex spheres/Dextran		SSRC/sucrose		SSRC/Dextran
	75 pM IgM	150 pM IgM	75 pM IgM	150 pM IgM	150 pM IgM
$30 \leq F_n < 85$	0.08 ( $n = 64$ )	0.06 ( $n = 61$ )	0.20 ( $n = 55$ )	0.12 ( $n = 77$ )	0.12 ( $n = 52$ )
$85 \leq F_n < 145$	0.16 ( $n = 84$ )	0.06 ( $n = 64$ )	0.60 ( $n = 25$ )	0.40 ( $n = 105$ )	0.20 ( $n = 35$ )
$145 \leq F_n < 205$	0.43 ( $n = 84$ )	0.20 ( $n = 73$ )	—*	0.47 ( $n = 78$ )	0.33 ( $n = 63$ )
$205 \leq F_n < 265$	0.57 ( $n = 58$ )	0.37 ( $n = 65$ )	—*	—*	—*

All comparisons between columns are significantly different.

$n$ , Number of doublets.

\*No data.

for formation of a bond; 4)  $\langle N_b \rangle$ , the average number of bonds. Simulations of the first 10 rotations were performed with normal forces corresponding to the mean values in each of the antigen sphere force ranges: 55 pN, 115 pN, 175 pN, and 235 pN. Five sets of 100 doublets were simulated, and the average and standard deviation of the fraction of break-ups per rotation,  $\langle N_r \rangle$ , and total fraction broken within 10 rotations were determined. Simulations were run with  $c$  from  $10^8$  to  $10^{13}$  N $^{-1}$ ,  $t_o$  from 1 to  $10^5$  s,  $t_f$  from 0.01 to 100 s, and  $\langle N_b \rangle$  from 1 to 15 bonds.

The best fit to the fraction of break-ups per rotation of the antigen spheres was determined by computing a  $\chi^2$  statistic for the first four rotations (because the number of break-ups used to compute the higher rotation number values is small) at each of the above  $F_n$ . The results of a comprehensive survey of the four parameters showed that a good match to the antigen sphere data could be found by using  $c = 3 \times 10^{10}$  N $^{-1}$ ,  $t_o = 25$  s,  $t_f = 2$  s. The fraction of break-ups per rotation for the four simulated forces are plotted in Fig. 4, *a* and *b*, and the aggregate statistics are given in Table 7.

The 75-pM antigen sphere data (Fig. 2 *a*) were well matched with a Poisson distribution of bonds having a mean  $\langle N_b \rangle = 1$  (Fig. 4 *a*). The observed fractions of break-up in the first rotation were well reproduced by the simulated curves, as was the slow decrease for  $F_n = 175$  pN and 235 pN. At 150 pM IgM, more bonds would be expected to form, and hence, the only parameter that should change is  $\langle N_b \rangle$ . Indeed, using the same  $c$ ,  $t_o$ , and  $t_f$ , it is found that the 150 pM antigen sphere data (Fig. 2 *b*) were quite well matched with  $\langle N_b \rangle = 2.5$  (Fig. 4 *b*), although the simulated decrease in break-up in the two highest force ranges is too rapid, and the values at longer times are too low.

The observed fraction of break-up within 10 rotations is also well matched at both [IgM]: the ratio of the simulated to observed values is always  $< 1.5$ , and averages over the four force ranges are 1.13 and 0.98 at 75 and 150 pM, respectively. The ratio of simulated to observed average number of rotations to break-up is always less than 1.38,

and the means over the four force ranges are 1.16 and 1.17 at 75 and 150 pM, respectively.

It proved impossible to find a better fit to the statistics derived from the antigen sphere experiments. In

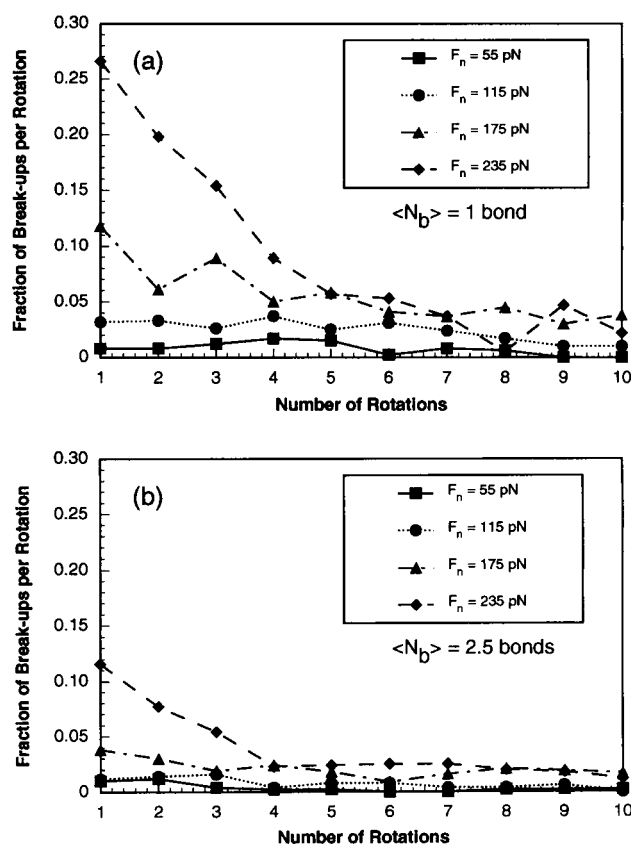


**FIGURE 4** Graph of the simulated fraction of break-ups per rotation for  $F_n = 55, 115, 175$ , and  $235$  pN produced by computer simulation of shear-induced rotation of doublets. The best-fit parameters of the stochastic model were  $c = 3 \times 10^{10}$  N $^{-1}$ ,  $t_o = 25$  s,  $t_f = 2$  s, with the mean value of the Poisson distribution in number of bonds,  $\langle N_b \rangle =$  (a) 1, (b) 2.5 corresponding to the experiments in 75 pM and 150 pM IgM, respectively.

**TABLE 7** Comparison of measured and simulated fraction of doublets and average number of rotations for doublets broken up within 10 rotations

Applied force (pN)	$\langle N_r \rangle \pm \text{SD}, s$					
	75 pM*	$\langle N_b \rangle = 1^{\#}$	Ratio	150 pM*	$\langle N_b \rangle = 2.5^{\#}$	Ratio
$30 \leq F_n < 85$	$3.6 \pm 2.2$	$3.8 \pm 1.9$	1.06	$1.8 \pm 2.4$	$2.6 \pm 2.2$	1.22
$85 \leq F_n < 145$	$2.6 \pm 1.7$	$3.6 \pm 2.5$	1.38	$2.7 \pm 1.2$	$3.5 \pm 2.6$	1.30
$145 \leq F_n < 205$	$2.4 \pm 2.2$	$3.2 \pm 2.8$	1.33	$3.0 \pm 2.4$	$3.8 \pm 3.0$	1.27
$205 \leq F_n < 265$	$2.2 \pm 2.0$	$1.9 \pm 2.1$	0.86	$2.8 \pm 1.7$	$2.5 \pm 2.6$	0.89
			(1.16)			(1.17)
Fraction of Break-ups						
$30 \leq F_n < 85$	0.08	0.07	0.88	0.06	0.04	0.67
$85 \leq F_n < 145$	0.15	0.22	1.47	0.06	0.08	1.33
$145 \leq F_n < 205$	0.43	0.45	1.05	0.20	0.18	0.90
$205 \leq F_n < 265$	0.57	0.64	1.12	0.32	0.33	1.03
			(1.13)			(0.98)

\*Measured values in suspensions containing 75 or 150 pM IgM antibody.

<sup>#</sup>Simulated values with a Poisson distribution of bonds having the mean values  $\langle N_b \rangle$  shown.

some cases, it was possible to find initial values of the fraction of break-ups per rotation that closely matched the data, but in all such cases, the simulated decrease in break-up with time was either too fast or too slow. As previously noted (Tees et al., 1993), because of the decrease in duration of shear in each orbit with increasing shear rate, for  $c < 2.5 \times 10^{10} \text{ N}^{-1}$  the fraction of break-up per rotation actually decreased with increasing force. For  $c > 5 \times 10^{11} \text{ N}^{-1}$ , there is almost immediate break-up in all force ranges; for  $c > 3.5 \times 10^{10} \text{ N}^{-1}$ , the fractions of break-up per rotation values in the second and third rotations are always too small (i.e., the decline is too precipitous). The search for the best fit of the antigen data was, therefore, concentrated in the region  $2.5 \leq c \leq 3.5 \times 10^{10} \text{ N}^{-1}$ . Using this range of  $c$ , simulation showed that the best fit must lie between  $20 \leq t_o \leq 50 \text{ s}$ , and  $\langle N_b \rangle$  must be very small ( $< 2$  bonds to fit the 75 pM data). At values of  $t_f < 1 \text{ s}$ ,  $t_o$  or  $\langle N_b \rangle$  must become even smaller to fit the data. As  $t_f$  increases to 100 s (effectively infinite, because the probability of formation of a single bond in the maximum 10 s required to complete 10 rotations is only 0.1), the fit remains relatively good (Tees, 1995). A formation time of 2 s seems rather short to be consistent with an initial  $\langle N_b \rangle$  of 1 bond, given that doublets are usually given many minutes to form bonds before they are sheared. It is possible that a better fit with a greater  $t_f$  exists; however, the parameter limits above are insensitive to changes in  $t_f$  if  $t_f > \sim 1 \text{ s}$ . Because no search of parameter space can ever be completely exhaustive, the parameters here may not correspond to the absolute best fit, but it is clear that the best fit value must lie nearby.

An attempt was made to fit the antigen sphere data using the formula suggested by Evans (Eq. 2). In spite of the three parameters ( $\tau_o$ ,  $f_o$ , and  $a$ ) used in the equation as formulated, this is actually a two-parameter model,  $t_b = t_e f^{-a}$ , where  $t_e = \tau_o f_o^a$ . Substituting this equation into Eq. 8, the simulation can be performed as before. Using  $a$  from 1 to 5,  $t_e$  from  $10^{-3}$  to  $10^4$ ,  $t_f$  from  $10^{-2}$  to  $10^2$ , and  $\langle N_b \rangle$  from 1 to 9, no

satisfactory fit was found. Although parameter combinations with  $a \approx 3$  could match the initial values well, the fraction of break-ups per rotation remained constant with time, whereas it should have decreased, and consequently, the fraction of break-up within 10 rotations was far too high.

### Bond parameters: SSRC versus antigen-linked spheres

Using the best-fit values of  $c = 3 \times 10^{10} \text{ N}^{-1}$ ,  $t_o = 25 \text{ s}$ ,  $t_f = 2 \text{ s}$ , and  $\langle N_b \rangle = 1$  (for the 75 pM data) and 2.5 (for the 150 pM data), one obtains from Bell's theory values of  $E_o = 0.8 \text{ eV}$  (assuming  $\tau_o = 10^{-13} \text{ s}$ ) and  $r_o = 0.12 \text{ nm}$ . The critical force,  $f_c$ , required to completely eliminate the energy minimum for a single bond ( $= E_o/r_o$ ) is then  $\sim 1000 \text{ pN}$ .

In the previous paper, the same simulation, but without a formation time, was applied to analyze the break-up of SSRC at 75 pM. The SSRC data have been resimulated for the three SSRC forces (55, 111, and 167 pN) with the formation time added. No better fit has been found, however, than that previously obtained (with  $t_f = \infty$ ; see Tees et al., 1993) using  $c = 1 \times 10^{11} \text{ N}^{-1}$ ,  $t_o = 100 \text{ s}$ ,  $t_f = 100 \text{ s}$ , and  $\langle N_b \rangle = 4$  for the 150 pM data. The corresponding bond parameters are  $E_o = 0.9 \text{ eV}$ ,  $r_o = 0.4 \text{ nm}$ , and  $f_c = E_o/r_o \approx 360 \text{ pN}$ .

Because  $t_o = \tau_o \exp(E_o/kT_K)$ , the depth of the bond energy minimum,  $E_o$ , is relatively insensitive to variation in  $t_o$ , which explains why  $E_o$  is very similar for both antigen spheres and SSRC, in spite of the fourfold difference in  $t_o$  found for the two systems. The calculation of  $E_o$  requires the value of  $\tau_o$ , the reciprocal of the natural frequency of oscillation of atoms in solids. This quantity is estimated to be anywhere from  $10^{-13}$  to  $10^{-8} \text{ s}$  (Bell, 1978). The calculation here uses  $10^{-13} \text{ s}$ , and the values will decrease if  $\tau_o$  is larger (to  $\sim 0.6 \text{ eV}$  for SSRC at  $10^{-8} \text{ s}$ ). The average number of bonds is very small in both systems, although it

is somewhat smaller ( $\langle N_b \rangle = 2.5$ ) for the antigen spheres than for the SSRCs ( $\langle N_b \rangle = 4$ ) at 150 pM IgM. The principal difference between the antigen spheres and the SSRCs is in  $r_o$ , the range of the bond. The  $r_o$  for the antigen spheres is  $\sim 3$  times smaller than that for the SSRCs. This implies that the bond being broken in the antigen sphere experiments is much less responsive to force than was the one studied in the previous paper using SSRC, a result similar to that found by others for the selectin-carbohydrate bond with  $r_o = 0.05$  nm (Alon et al., 1995), who suggested that the range of such a bond was comparable to that for hydrogen bonding (in contrast to protein-protein interactions, which are hydrophobic and have longer ranges). Thus the antibody-blood group B antigen bond (which is also a protein-carbohydrate bond) exhibits a "high tensile strength" (using the language of Alon et al., 1995) or a low reactive compliance (to use the language of Hammer and Apte, 1992). It should be noted, however, that although  $r_o$  has the dimensions of length, and is thought to be on the order of the size of the receptor-ligand binding cleft (Bell, 1978), it is in fact only a parameter describing the dependence of bond lifetime on force. The value may, in principle, be much less than the physical dimensions of the binding cleft, a situation that must apply here, because  $r_o \approx 1$  Å corresponds to the size of a hydrogen atom, which seems implausibly small for a binding cleft width.

The simulation allows the effect of bond number and bond strength to be separated. The results for the antigen spheres and SSRC show that the difference in time and force dependence of break-up is due to a difference in the character of the bond, not in the number of bonds cross-linking doublets. The difference in the bond character suggests that a different mode of rupture of the bond is being examined (i.e., receptor extraction versus antigen-antibody bond breakage), although other effects due to the different chemical neighborhoods of the bonds on SSRC versus antigen spheres cannot be excluded.

### Effect of viscosity

The significant difference seen between the 19% and 15% Dextran 40 break-up statistics showed that there is an effect of viscosity on the aggregation of antigen spheres. Doublets of spheres were significantly easier to break up in 19% Dextran ( $\eta_{23^\circ\text{C}} = 18.3$  mPa·s) than in 15% Dextran ( $\eta_{23^\circ\text{C}} = 9.7$  mPa·s) at both [IgM]. Furthermore, as noted above, the similarity between the break-up fractions in 75 pM/15% Dextran and the 150 pM/19% Dextran is curious and suggests that the increased break-up is due to a decreased number of bonds in the more concentrated Dextran, rather than a change in the character of the bond. This could be consistent with an increased adsorption of Dextran to the spheres, blocking more antigen sites in 19% than in 15% Dextran.

One possible explanation for the difference is that at higher viscosity, a lower shear rate is required to achieve a

given force. The reduced  $G$  corresponds to a longer  $T$ , and thus a doublet spends a longer time in each rotation exposed to a given force. Computer simulation of the lower viscosity experiments that explored this effect, however, showed only a  $\sim 30\%$  decrease in fraction of break-up over the three lower force ranges, not the 50% decrease required, so this effect can only account for part of the difference. Simulation of break-up at the highest force range showed no significant decrease in the fraction of break-up.

The viscosity effect is also apparent in the results of a population study of formation of antibody-linked antigen sphere aggregates. Latex spheres at a concentration of  $2 \times 10^4$  spheres  $\mu\text{l}^{-1}$  were sheared in a thermostatted cone and plate viscometer (Brookfield Engineering Laboratories, Can-Am Instruments, Mississauga, ON, Canada) at  $25^\circ\text{C}$  with 1.9 nM anti-B antibody in 5, 10, 15, and 20% Dextran 40 ( $\eta = 2.2, 5.0, 10.3$ , and  $19.7$  mPa·s, respectively). For each series of viscosities, the sphere suspensions were exposed either to constant shear rate ( $G = 23.0$  s $^{-1}$ ) or to constant force (by reducing  $G$  from  $46.0$  to  $5.8$  s $^{-1}$  to compensate for the increased viscosity at the higher [Dextran]). The size distribution of aggregates in a sample of suspension taken at 24 h (by which time the degree of aggregation had been found to have reached an equilibrium value) was determined under the microscope. The average number of spheres in aggregates and the percentage of spheres in aggregates are plotted in Fig. 5, *a* and *b*, as a function of viscosity at both constant shear rate and constant force. As viscosity increased, the percentage of spheres in aggregates decreased steadily. The average size of aggregates, by contrast, decreased rapidly at first, but leveled off by 10 mPa·s, because of the disappearance of very large aggregates. In addition, there was no significant difference between the constant force and constant shear rate curves (perhaps because the applied forces were  $< 55$  pN). The similarity between the constant shear rate data (for which break-up is expected to be viscosity dependent because of the increased applied force with increasing viscosity) and the constant force data (for which break-up is not expected to vary with viscosity because the force does not increase) implies that formation dominates over break-up in the decrease of aggregate size with increasing viscosity. At low viscosity, large numbers of bonds can form, resulting in very large aggregates, whereas at high viscosity, the bond number should decrease.

The large density differences between latex spheres and 52% sucrose and its attendant rapid sedimentation required the substitution of Dextran as a suspending medium for the antigen sphere experiments. To ensure that viscosity would not affect the comparison, the viscosity of the Dextran suspending medium was matched to that of 52% sucrose. There remains a question, however, of whether the nature of the viscous cosolvent used can affect the antigen-antibody interaction. The effect of suspending medium on SSRC doublet break-up was examined directly by repeating the experiments in 52% sucrose, using 19% Dextran 40 as the suspending medium. As shown in Table 6, the SSRC results

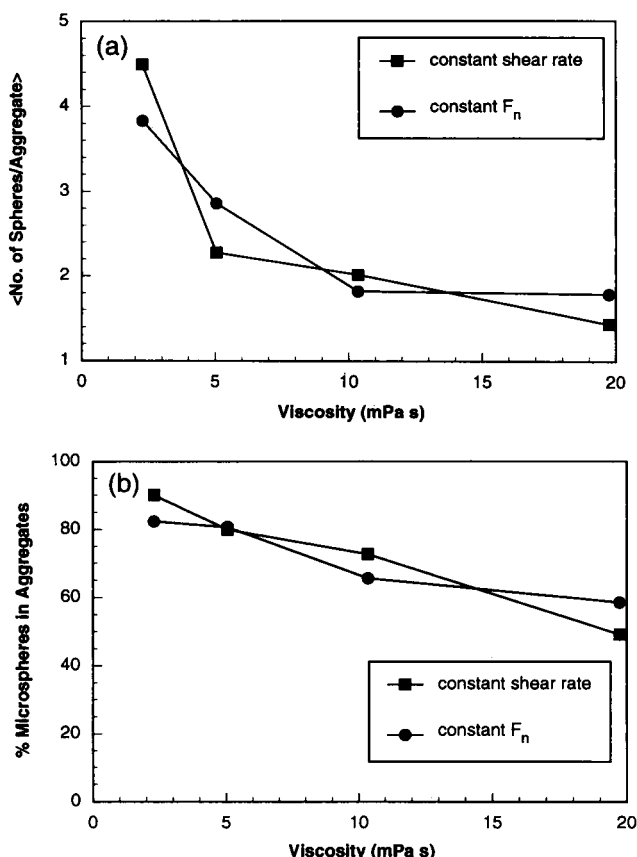


FIGURE 5 Population study of aggregate formation. Plots of (a) average number of spheres per aggregate and (b) percentage of microspheres in aggregates when  $2 \times 10^4$  spheres  $\mu\text{l}^{-1}$  with 1.9 nM anti-B antibody in 5, 10, 15, and 20% Dextran 40 ( $\eta = 2.2, 5.0, 10.3, \text{ and } 19.7$  mPa s at  $25^\circ\text{C}$ , respectively) were exposed to either constant shear rate or constant force for each viscosity series in a cone and plate viscometer.

in Dextran differ from those in sucrose, but not enough to account for the difference between SSRC and latex spheres. A lingering concern, however, is whether the change in the chemical environment of the antigen-antibody bond due to the change from lipid bilayer with glycocalyx to CML sphere with its three-dimensional surface coat of carboxyl groups could have accounted for the difference.

### Effect of pH

The pH of the suspending medium has an effect on the time and force dependence of antigen sphere doublet break-up. The fraction of break-up increased as pH decreased from 7.8 to 7.1 (indicating a weakening of the bond), a result that is to be expected as the pH decreases toward the pK of the antigen-antibody system. At pH 5.8, however, there was very little break-up at all. One hypothesis for this unusual behavior is that bonds were so weak at this pH that very few doublets formed in the rheoscope, and those that were analyzed were actually the preexisting, tenaciously bound, nonspecific doublets (of which there were always one or two per rheoscope filling). However, this hypothesis could

not be substantiated, because population studies of [doublets] within the rheoscope showed no change with pH. It is possible that a conformational change caused by titration of key amino acids within the binding site that are involved in binding and structure stabilization could be responsible for all of the pH effects.

### CONCLUSION

The objective of this paper was to couple an antigen covalently to latex microspheres, to ensure that an antigen-antibody bond was being ruptured during the break-up of antibody agglutinated antigen-sphere doublets. The time distribution of break-up as a function of force was compared with that for SSRC to determine whether in the latter case the antigen is being extracted from the membrane. Evidence has been presented here that shows the doublets of blood group B antigen-linked spheres are significantly harder to break up than type B sphered, swollen red cells in the presence of equal amounts of the same cross-linking anti-B antibody, consistent with antibody-antigen bond rupture versus receptor extraction. The difference is reflected in the results of the computer simulation, which shows that the increased resistance to break-up is not due to an increase in the number of bonds, but to a change in bond parameters.

Evidence for a decrease in the amount of binding with increasing viscosity of the suspending medium has also been presented. The time per rotation spent under stress, caused by the decreased shear rate required to reach a given force at lower viscosity, can only account for about half of the observed difference. A decrease in the number of bonds with increasing [Dextran 40], which could explain much of the rest of the discrepancy, could be due to absorption of Dextran onto the spheres and the consequent blockage of antigen sites.

Clearly, the viscosities must be matched for the SSRC and antigen sphere doublet break-ups to be comparable, and this has been done. Notwithstanding the explanations just mentioned, there remains the question of whether the nature of the viscous cosolvent in the medium [sucrose versus Dextran (polysucrose)] might also affect adhesion because of solvent exclusion effects. Population studies of aggregate formation suggest that there is an effect of suspending medium, although because of differing rates of sedimentation, the results of the two experiments are not strictly comparable. Repeating the SSRC studies in Dextran, however, showed that this effect could not account for the differences between the SSRC and latex sphere results, although the role of the change in chemical environment caused by the shift from cell to CML receptor substrates is unclear.

Above these considerations looms the possibility that receptors covalently linked to latex spheres may be extracted from microspheres. Extraction of latex strands from microspheres has been reported (Dabros et al., 1994) and remains an issue for all receptor-ligand experiments using

microspheres with a relatively low degree of polymer cross-linking. Given, however, that CML doublet break-up is pH dependent, the extraction hypothesis is rendered less likely for these spheres, and it seems plausible that an antigen-antibody bond is indeed being broken.

In this paper we have attempted to characterize the force dependence of adhesion for a protein-carbohydrate bond. In the companion paper (Part II), again using latex spheres, we describe similar experiments to characterize the force dependence of adhesion for a protein-protein bond.

We gratefully acknowledge Fiona McIntosh for her expert technical assistance, and Dr. Joyce Rauch and Rebecca Subang for their assistance in performing the ELISA. We also wish to thank Drs. Pierre Wong, Gerald Price, Stan Lam, Susan Tha, and Theo van de Ven for useful discussions.

This work was supported by grant MT 1835 from the Medical Research Council of Canada.

## REFERENCES

- Almagor, A., S. Yedgar, and B. Gavish. 1992. Viscous cosolvent effect on the ultrasonic absorption of bovine serum albumin. *Biophys. J.* 61: 480–486.
- Alon, R., D. A. Hammer, and T. A. Springer. 1995. Lifetime of the P-selectin-carbohydrate bond and its response to tensile force in hydrodynamic flow. *Nature*. 374:539–542. (Correction 1995. 377:86)
- Bell, G. I. 1978. Models for the specific adhesion of cells to cells. *Science*. 200:618–627.
- Bevington, P. R. 1969. *Data Reduction and Error Analysis for the Physical Sciences*. McGraw-Hill, New York.
- Capo, C., F. Garrouste, A.-M. Benoliel, P. Bongrand, A. Ryter, and G. I. Bell. 1982. Concanavalin-A-mediated thymocyte agglutination: a model for a quantitative study of cell adhesion. *J. Cell Sci.* 56:21–48.
- Cozens-Roberts, C., J. A. Quinn, and D. A. Lauffenburger. 1990. Receptor-mediated adhesion phenomena: model studies with the radial flow detachment assay. *Biophys. J.* 58:107–125.
- Dabros, T., P. Warszynski, and T. G. M. van de Ven. 1994. Motion of latex spheres tethered to a surface. *J. Colloid Interface Sci.* 162:254–256.
- Dembo, M., D. C. Torney, K. Saxman, and D. Hammer. 1988. The reaction limited kinetics of membrane-to-surface adhesion and detachment. *Proc. R. Soc. Lond. B. Biol. Sci.* 234:55–83.
- Erickson, H. P. 1994. Reversible unfolding of fibronectin type III and immunoglobulin domains provides the structural basis for stretch and elasticity of titin and fibronectin. *Proc. Natl. Acad. Sci. USA*. 91: 10114–10118.
- Evans, E. 1993. Microscopic-physical determinants in biological adhesion. *Blood Cells*. 19:401–419.
- Evans, E., D. Berk, and A. Leung. 1991. Detachment of agglutinin-bonded red blood cells. I. Forces to rupture molecular-point attachments. *Biophys. J.* 59:838–848.
- Goldsmith, H. L., and S. G. Mason. 1967. The microrheology of dispersions. In *Rheology: Theory and Applications*, Vol. 4. F. R. Eirich, editor. Academic Press, New York. 85–250.
- Hammer, D. A., and S. M. Apte. 1992. Simulation of cell rolling and adhesion on surfaces in shear flow: general results and analysis of selectin-mediated neutrophil adhesion. *Biophys. J.* 63:35–57.
- Kaplanski, G., C. Farnier, O. Tissot, A. Pierres, A.-M. Benoliel, M.-C. Alessi, S. Kaplanski, and P. Bongrand. 1993. Granulocyte-endothelium initial adhesion: analysis of transient binding events mediated by E-selectin in a laminar shear flow. *Biophys. J.* 64:1922–1933.
- Kwong, D., D. F. J. Tees, and H. L. Goldsmith. 1996. Kinetics and locus of failure of receptor-ligand-mediated adhesion between latex spheres. II. Protein-protein bond. *Biophys. J.* 71:1115–1122.
- Lawrence, M. B., and T. A. Springer. 1991. Leukocytes roll on a selectin at physiological flow rates: distinction from and prerequisite for adhesion through integrins. *Cell*. 65:859–874.
- Lemieux, R. U., D. R. Bundle, and D. A. Baker. 1975. Properties of "synthetic" antigen related to the human blood-group Lewis a. *J. Am. Chem. Soc.* 97:4076–4083.
- Lemieux, R. U., and H. Driguez. 1975. The chemical synthesis of 2-O-( $\alpha$ -L-fuco-pyranosyl)-3-O-( $\alpha$ -D-galactopyranosyl)-D-galactose. The terminal structure of the blood-group B antigenic determinant. *J. Am. Chem. Soc.* 97:4069–4075.
- Pierres, A., A.-M. Benoliel, and P. Bongrand. 1995. Measuring the lifetime of bonds made between surface-linked molecules. *J. Biol. Chem.* 270: 26586–26592.
- Press, W. H., B. P. Flannery, S. A. Teukolsky, and W. T. Vetterling. 1986. *Numerical Recipes*. Cambridge University Press, New York.
- Sachs, L. 1984. *Applied Statistics: A Handbook of Techniques*, 2nd Ed. Springer-Verlag, New York. 367–369.
- Shaw, D. J. 1969. *Electrophoresis*. New York: Academic Press.
- Tees, D. F. J. 1995. On the time and force dependence of antigen-antibody mediated cell adhesion. Ph.D. thesis. McGill University, Montréal, Canada.
- Tees, D. F. J., O. Coenen, and H. L. Goldsmith. 1993. Interaction forces between red cells agglutinated by antibody IV. Time and force dependence of break-up. *Biophys. J.* 65:1318–1334.
- Tha, S. P., and H. L. Goldsmith. 1986. Interaction forces between red cells agglutinated by antibody. I. Theoretical. *Biophys. J.* 50:1109–1116.
- Tha, S. P., J. Shuster, and H. L. Goldsmith. 1986. Interaction forces between red cells agglutinated by antibody. II. Measurement of hydrodynamic force of breakup. *Biophys. J.* 50:1117–1126.
- van Oss, C. J., and D. R. Absolom. 1984. Nature and thermodynamics of antigen-antibody interactions. In *Molecular Immunology*. M. Z. Atassi, C. J. van Oss, and D. R. Absolom, editors. Marcel Dekker, New York. 337–360.
- Wakiya, S. 1971. Slow motion in shear flow of a doublet of two spheres in contact. *J. Phys. Soc. Jpn.* 31:1581–1587. (Errata. 1972. 33:278).
- Xia, Z., H. L. Goldsmith, and T. G. M. van de Ven. 1994. Flow-induced detachment of red blood cells adhering to surfaces by specific antigen-antibody bonds. *Biophys. J.* 66:1222–1230.